의학박사 학위논문

Prognostic implication of *Fibroblast growth factor receptor 1* (*FGFR1*) gene copy number alteration in colorectal cancers using droplet digital polymerase chain reaction (ddPCR)

비말 디지털 중합효소연쇄반응(droplet digital polymerase chain reaction)을 이용한 결장직장암에서의 제1형 섬유모세포성장 인자수용체(*Fibroblast growth factor receptor 1)* 유전자 복제수 변이의 예후 예측

2017년 2월

서울대학교 대학원

의학과 병리학 전공

배정모

비말 디지털 중합효소연쇄반응(droplet digital polymerase chain reaction)을 이용한 결장직장암에서의 제1형 섬유모세포성장인자수용체(*Fibroblast growth factor receptor 1*) 유전자 복제수 변이의 예후 예측

지도교수 강 경 훈

이 논문을 의학박사학위논문으로 제출함

2016 년 10 월

서울대학교 대학원

의학과 병리학 전공

배정모

배정모의 박사학위논문을 인준함

2017 년 1 월

위 원 장 _____ (인)

부위원장 _____ (인)

위 원 _____ (인)

위 원 _____ (인)

위 원 _____ (인)

Prognostic implication of *Fibroblast growth factor receptor 1* (*FGFR1*) gene copy number alteration in colorectal cancers using droplet digital polymerase chain reaction (ddPCR)

by

Jeong Mo Bae

A thesis submitted to the Department of Pathology in partial fulfillment of the requirements for the Degree of Doctor of Philosophy in Pathology at Seoul National University College of Medicine

JAN 2017

Approved by Thesis Committee:

Professor _____Chairman

Professor _____Vice Chairman

Professor_____

Professor_____

Professor_____

Abstract

Jeong Mo Bae

Department of Pathology, College of Medicine

The Graduate School

Seoul National University

Amplification *of Fibroblast grow factor receptor 1* (*FGFR1*) is reported in several types of cancers. However, the clinicopathologic characteristics and prognostic implication of *FGFR1* amplification in colorectal cancers (CRCs) are not well known. We measured copy number of *FGFR1* gene using droplet digital polymerase chain reaction (ddPCR) and FGFR1 expression using immunohistochemistry in 789 surgically resected CRCs (384 CRCs for discovery set and 405 CRCs for validation set). CRCs with *FGFR1* gene copy more than 3.15 were classified to *FGFR1* amplification and CRCs with moderate and strong FGFR1 expression were classified to FGFR1 high-expression.

FGFR1 amplification was found in 11 (2.9%) of 384 CRCs of discovery set and 32 (7.9%) of 405 CRCs of validation set. CRCs with *FGFR1* amplification showed

mutual exclusiveness with microsatellite instability and *BRAF* mutation. There was no predilection for sex, gross pattern, tumor location, stage and differentiation according to *FGFR1* copy number status. FGFR1 high-expression was found in 50 (13.1%) of 382 CRCs of discovery set and 62 (16.5%) of 375 CRCs of validation set. *FGFR1* amplification and FGFR1 high-expression did not show significant correlation. In the discovery set, CRCs with FGFR1 high-expression showed female preponderance, advanced N category and overall stage, frequent *KRAS* mutation and CIMP-high subtype. In survival analysis, CRCs with *FGFR1* amplification showed significantly worse clinical outcome compared with CRCs with *FGFR1* no-amplification in both discovery set and validation set. CRCs with FGFR1 high-expression showed worse progression-free survival compared with CRCs with FGFR1 low-expression only in the discovery set. FGFR inhibitor PD173074 repressed proliferation of CRC cell line with FGFR1 overexpression rather than CRC cell lines with *FGFR1* amplification.

In a conclusion, *FGFR1* amplification measured by ddPCR can be a prognostic indicator of poor clinical outcome in CRCs.

Keywords : colorectal cancer, *fibroblast growth factor receptor 1*, copy number alteration, droplet digital polymerase chain reaction, prognosis

Student Number : 2011-31147

Table of contents

Abstract ····· i

Contents ····· iii

List of Tables ····· iv

List of Figures ····· vi

List of Abbreviations ····· vii

Introduction ····· 1

Materials and methods ····· 4

Results ····· 12

Discussion ····· 39

Conclusion ····· 42

References ····· 43

Abstract in Korean ····· 47

List of Tables

Table 1. *FGFR1* gene status in ddPCR compared with FISH

Table 2. Clinicopathologic characteristics of CRCs according to the *FGFR1* amplification status (N = 384)

Table 3. Molecular characteristics of CRCs according to the *FGFR1* amplification status in the discovery set (N = 384)

Table 4. Clinicopathologic characteristics of CRCs according to the FGFR1 expression status in the discovery set (N = 382)

Table 5. Molecular characteristics of CRCs according to the FGFR1 expression status in the discovery set (N = 382)

Table 6. Clinicopathologic and molecular characteristics of CRCs according to the *FGFR1* amplification status in the validation set (N = 405)

Table 7. Clinicopathologic and molecular characteristics of CRCs according to the FGFR1 expression status in the validation set (N = 405)

Table 8. Univariate Cox proportional hazard model for 5-year disease-free survival in the validation set (N = 405)

Table 9. Multivariate Cox proportional hazard model for 5-year disease-free

survival in the validation set (N = 405)

List of Figures

Figure 1. Correlation of *FGFR1*/*RPPH1* ratio in ddPCR and *FGFR1*/CEP ratio in FISH

Figure 2. FGFR1 expression in colorectal cancers

Figure 3. Comparison of *FGFR1* copy and FGFR1 expression in the discovery set, validation set and TCGA COADREAD dataset

Figure 4. Mutual exclusiveness of the *FGFR1* amplification with microsatellite instability, *BRAF* mutation and CpG island methylator phenotype

Figure 5. Kaplan-Meier survival curves in the discovery set

Figure 6. Kaplan-Meier survival curves in the validation set

Figure 7. IC_{50} of PD173074 in four CRC cell lines

List of Abbreviations

CRC: colorectal cancer

FGFR1: *fibroblast growth factor receptor 1*

CIN: chromosomal instability

MSI: microsatellite instability

MSS: microsatellite stable

CIMP: CpG island methylator phenotype

ddPCR: droplet digital polymerase chain reaction

CNA: copy number alteration

FISH: fluorescence *in situ* hybridization

CISH: chromogenic *in situ* hybridization

SISH: silver-enhanced *in situ* hybridization

Introduction

Colorectal cancers (CRCs) are third-most commonly diagnosed malignancy in the US and South Korea.[1, 2] CRCs are developed by accumulation of genetic and epigenetic alterations, and recent comprehensive genomic and epigenomic analysis increased our understanding of genomic alterations in CRCs tremendously.[3] Although alternative carcinogenic pathways, such as microsatellite instability (MSI) and CpG island methylator phenotype (CIMP) have been described, the vast majority of CRCs (about 70%) are developed by chromosomal instability (CIN), which is characterized by accumulation of somatic mutations and copy number alterations.[4] In a functional aspect, CRCs are dominated by somatic mutations rather than copy number alterations.[5] However, several genomic regions show significant focal amplification or deletion in CRCs.[3]

Fibroblast growth factor receptor 1 (*FGFR1*) is a transmembrane receptor tyrosine kinase located in 8p11.[3] The FGFR family includes four receptor tyrosine kinases, FGFR1-4, and its structural variability is derived from alternative splicing.[6] FGFR ligands, fibroblast growth factors (FGFs) are known to activate downstream signaling pathways including mitogen-activated protein kinase and phosphoinositide-3-kinase/AKT. FGF signaling promotes cell proliferation, cell survival, and angiogenesis, resulting in tumor development.[7] Amplification of *FGFR1* gene is reported in ER-positive breast cancers, lung cancers, esophageal

cancers and bladder cancers. Recently, association of *FGFR1* amplification with poor prognosis has been suggested in various types of cancers, including squamous cell carcinoma of the lung and esophagus, ER-positive breast cancers.[8-10]

Fluorescence *in situ* hybridization (FISH) is considered to be a gold standard in the evaluation of copy number alterations (CNA) in clinical oncology.[11, 12] However, FISH has several disadvantages, such as requirement of fluorescence microscope and dark room, subjective measurement of fluorescence signal, spontaneous weakening of fluorescence along time and expensive price. Chromogenic *in situ* hybridization (CISH) and silver-enhanced *in situ* hybridization (SISH) have been developed to overcome limitations of FISH caused by using fluorescence.[13, 14] However, subjectivity caused by visual inspection still remains in CISH and SISH. Although quantitative measurement of nucleic acids using polymerase chain reaction (PCR) has been considered an alternative method for CNA analysis, quantitative real-time PCR is not widely used in clinical practice due to low reproducibility. Recently, water-oil emulsion droplet technology based third generation PCR technology, which called droplet digital PCR (ddPCR), is developed and ddPCR offers a number of advantages for both detecting and quantifying nucleic acids, such as fold-change measurements and rare variant detection.[15]

In CRCs, *FGFR1* amplification is found in 2 to 5%.[16, 17] However, clinicopathologic characteristics and prognostic implication of *FGFR1*

amplification in CRCs are not well known due to the scarcity of this alteration. In this study, we evaluated copy number of *FGFR1* in CRCs using ddPCR, and aimed to reveal clinicopathologic characteristics and prognostic implication of the *FGFR1* amplification.

Materials and Methods

Patient selection

Discovery set: A total of 538 patients with colorectal cancers underwent surgical treatment at Seoul National University Hospital between Jan 2007 to Dec 2007. After the exclusion of patients who refused to participate in the molecular study, or had non-invasive cancers, a neo-adjuvant treatment history, familial adenomatous polyposis, multiple tumors or recurrent tumors, 384 patients were subjected to clinicopathologic and molecular analysis.

Validation set: to validate survival analysis results from discovery set, we obtained tissues from 405 high-risk stage II or stage III colorectal cancer patients who received adjuvant FOLFOX during Aug 2005 to Dec 2011. Patients who fulfilled the inclusion criteria for the discovery set were excluded. This study was approved by Institutional Review Board.

Extraction of genomic DNA

DNA was extracted from formalin-fixed, paraffin-embedded tumor specimens. The

area in which tumor cells were most dense were delineated by light microscopy of the tissue sections. The corresponding areas were marked on 10 serial unstained slides. DNA extraction was performed after macro-dissection using ZR FFPE DNA MiniPrep™ (Zymo Research, Orange, CA, USA) according to the manufacturer's protocol.

Droplet digital PCR

Droplet digital polymerase chain reaction (ddPCR; QX200, Bio-Rad, Hercules, CA, USA) was used in this study. Each sample was partitioned into 20,000 droplets, with target and background (reference) DNA randomly, but not uniformly, distributed among the droplets. The following primers were used for ddPCR; *FGFR1*: Hs02882334_cn (LifeTechnologies®), *RPPH1*-ddF: 5'-GCGGATGCCTCCTTTGC-3', *RPPH1*-ddR – 5'-ACCTCACCTCAGCCATTGAACT-3', *RPPH1*-HEX: HEX-CTTGGAACAGACTCACGGCCAGCG-BHQ1. The reactions were performed in 20 μL reaction volumes that consisted of up to 100 ng of extracted DNA (5 μL), 2x ddPCR supermix for probe (10 μL), *FGFR1* primer (1 μL), *RPPH1* primer (1.8 μL), RPPH1-HEX (0.5 μL), HindIII (0.3 μL), and deionized distilled water (1.4 μL). The emulsified PCR reactions were run in a 96-well plate on a thermal cycler. The plates

were incubated at 95 °C for 10 min, followed by 50 cycles of 94 °C for 30 s, 60 °C for 50 s, 72 °C for 30 s and a 10 min incubation at 98 °C. The plates were read on a Bio-Rad QX200 droplet reader using the QuantaSoft v1.7 software (Bio-Rad) to assess the number of droplets positive for *FGFR1* and/or *RPPH1*. *FGFR1* gene copy number with ddPCR was defined 2 x *FGFR1*/*RPPH1*. Cut-off for *FGFR1* amplification was determined to ≥ 3.15 copies/cell (*FGFR1*/*RPPH* ≥ 1.575) by maximally selected chi-square statistics.

Tissue microarray construction and immunohistochemistry

Through histological examination, we marked portions that represent the tumor area for each patient sample. A pair of 2-mm core tumor tissues was subsequently extracted from each paraffin-embedded formalin tissues (donor block) and rearranged in a new recipient tissue microarray block using a trephine apparatus as previously described. To analyze FGFR1 expression, immunohistochemical analysis was performed with commercially available rabbit monoclonal anti-FGFR1 antibody (clone EPR806Y, abcam, 1:50). We evaluated the staining intensity of the cytoplasmic or membranous FGFR1 staining as 0 (no stain), 1 (mild stain), 2 (moderate stain), or 3 (strong stain). The level of FGFR1 expression were subsequently categorized as FGFR1-low (FGFR1 intensity 0 and 1), and FGFR1-

high (FGFR1 intensity 2 and 3) groups.

KRAS & *BRAF* mutation

After extraction of the genomic DNA, *KRAS* exon 2 was amplified by hemi-nested PCR (with rTaq DNA Polymerase, Takara, Kyoto, Japan) with the following primer set: forward primer (5′-ACTGAATATAAACTTGTGGTAGTTGGCCCT-3′), reverse primer 1 (5′-TAATATGTCGACTAAAACAAGATTTACCTC-3′), and reverse primer 2 (5′-TCAAAGAATGGTCCTGGACC-3′). The first PCR reaction mixture consisted of a 20 μL volume and contained the following: forward primer and reverse primer 1 with a concentration of 400nM, 1 x rTaq PCR buffer, 3 mM $MgCl_2$, 0.625 U of rTaq polymerase, 400 μM of each deoxynucleotide, and 100 ng of genomic DNA. The PCR reaction condition were as follows: 95 °C initial denaturation, 25 cycles of amplification (denaturation at 94 °C for 30 s, annealing at 55 °C for 40 s, and extension at 30 s at 72 °C for primer extension), and a final extension step at 72 °C for 10 min. One microliter of the first PCR product was used for the second PCR, which was conducted in a 25 μL volume containing 1 x PCR buffer (16.6 mM$(NH_4)_2SO_4$; 67 mM Tris, pH 8.8; 6.7 mM $MgCl_2$; and 10 mM β-mercaptoethanol), dNTP (each 1 mM), and primers (0.4 μM each of forward primer and reverse primer 2). Amplifications were performed in a thermal cycler for 35

cycles (30 s at 95 °C, 40 s at 57 °C, and 30 s at 72 °C) and were allowed a final 10-min extension at 72 °C. Five microliters of PCR product was treated with 1.2 U of shrimp alkaline phosphatase and 6 U of exonuclease in a final volume of 10 μL; PCR products were incubated at 37 °C for 15 min and then heat-inactivated at 80 °C for 15 min. The purified PCR products were sequenced with BigDye Terminator v3.1 cycle sequencing kit (Applied Biosystems, Foster City, CA, USA) and analyzed with a 3730 ABI capillary electrophoresis system (Applied Biosystems). All somatic mutations that were found were further validated by a new independent amplification and sequencing experiment. *BRAF* mutations at codon 600 (V600E) were analyzed by a real-time PCR-based allelic discrimination method, as previously described.

Microsatellite instability analysis

The microsatellite status of each tumor was determined through an evaluation of five microsatellite markers (D2S123, D5S346, D17S250, BAT25, and BAT26). A fluorescent label was added to either the forward or the reverse primer for each marker, and the PCR products were electrophoresed and analyzed. We classified MSI status as follows: MSI-high (instability at ≥ 2 microsatellite markers), MSI-low (instability at 1 marker), or microsatellite stable (MSS, no instability).

Methylation analysis

After sodium bisulfite conversion of DNA using an EZ DNA methylation kit (Zymo Research), the methylation status was quantified using a MethyLight assay in the following eight CIMP markers: *CACNA1G, CDKN2A*, *CRABP1*, *IGF2*, *MLH1*, *NEUROG1*, *RUNX3*, and S*OCS1*. The primer sequences and polymerase chain reaction (PCR) conditions have been previously described. *M*.SssI-treated genomic DNA was used as a reference sample. The percentage of methylated reference (PMR) at a particular locus was calculated by 100 x (methylated reaction at the GENE/control reaction at the ALU ratio)$_{sample}$ / (methylated reaction at the GENE/control reaction at the ALU)$_{M.SssI\text{-}treated\ placental\ genomic\ DNA}$. The MethyLight assay was repeated in triplicate, and of the three measured values, the median was regarded as a representative value of methylation level of each marker. A CpG island locus with a median PMR > 4 was considered to be methylated. CIMP status was defined according to the number of methylated markers, as follows: CIMP-high (methylation at ≥ 5 markers), CIMP-low (1–4 markers), or CIMP-0 (0 markers).

Cell proliferation assay

Three CRC cell lines with *FGFR1* amplification (SNU-C1, SNU-283 and SW620), one CRC cell line with FGFR1 high-expression (HCT116) and one CRC cell line with *FGFR1* no-amplification and FGFR1 low-expression (SNU-81) were grown for 72 h in RPMI-1640 or DMEM medium containing 10 % fetal bovine serum, at 37 °C under a humidified 5 % CO2 atmosphere. The effect of FGFR inhibitor PD173074 on cell proliferation was determined by the 3-(4,5-dimethylthiazol-2-yl)-2-5-diphenyltetrazolium bromide (MTT) cell viability assay in SNU-283, SW620, HCT116 and SNU-81.[18] For SNU-C1, WST-1 assay was performed. For MTT assay, after indicated treatment, 50 μL MTT reagent (5 mg/mL) was added per well for 4 h at 37 °C. Next, 150 μL of DMSO was added to lyse the cells and solubilize colored crystals. Plates were then incubated for 10 min at 37 °C. Optical density (OD) was obtained using a microplate reader at 570 nm wavelength. For WST-1 assay, after indicated treatment, 20 μL of WST-1 solution was added per well for 4 h at 37 °C. OD was obtained at 440nm wavelength. Half maximal inhibitory concentrations (IC_{50}) were calculated with SigmaPlot 13.

Public data analysis

Molecular characteristics of TCGA COADREAD dataset including copy number alteration and mRNA expression status of *FGFR1*, *BRAF* mutation, MSI and CIMP

status were obtained from cBioPortal for cancer genomics (http://cbioportal.org).[19]

Statistical analysis

Categorical variables were compared by $\chi 2$-test, Fisher's exact test or ANOVA test as appropriate. Progression-free survival, disease-free survival and overall survival was calculated using the log-rank test with Kaplan-Meier curve. Hazard ratios (HRs) were calculated using the Cox proportional hazard model. The assumption of proportional hazards was verified by plotting the log(-log(S(t)) against the time of the study. In the modeling process, all variables that were associated with DFS or OS with a $P < 0.10$ were entered into an initial model; these variables were then reduced by backward elimination. All statistical tests were two-sided, and statistical significance was defined as $P < 0.05$.

Results

Comparison of *FGFR1* gene copy measured by ddPCR and FISH

To test the compatibility of ddPCR with FISH in copy number analysis, we measured *FGFR1* gene copy using ddPCR in 20 FFPE CRC samples which are already evaluated *FGFR1* gene copy using FISH.[20] ddPCR and FISH results showed strong correlation (Spearman's rho: 0.686, $P = 0.001$) (Figure 1). Using cut-offs of ≥ 3.15 *FGFR1* copies/cell for ddPCR and $\geq$ *2 FGFR1*/CEP8 for FISH, ddPCR and FISH showed strong concordance for *FGFR1* amplification ($\kappa = 0.875$) (Table 1).

Figure 1. Correlation of *FGFR1*/*RPPH1* ratio in ddPCR and *FGFR1*/CEP8 ratio in FISH.

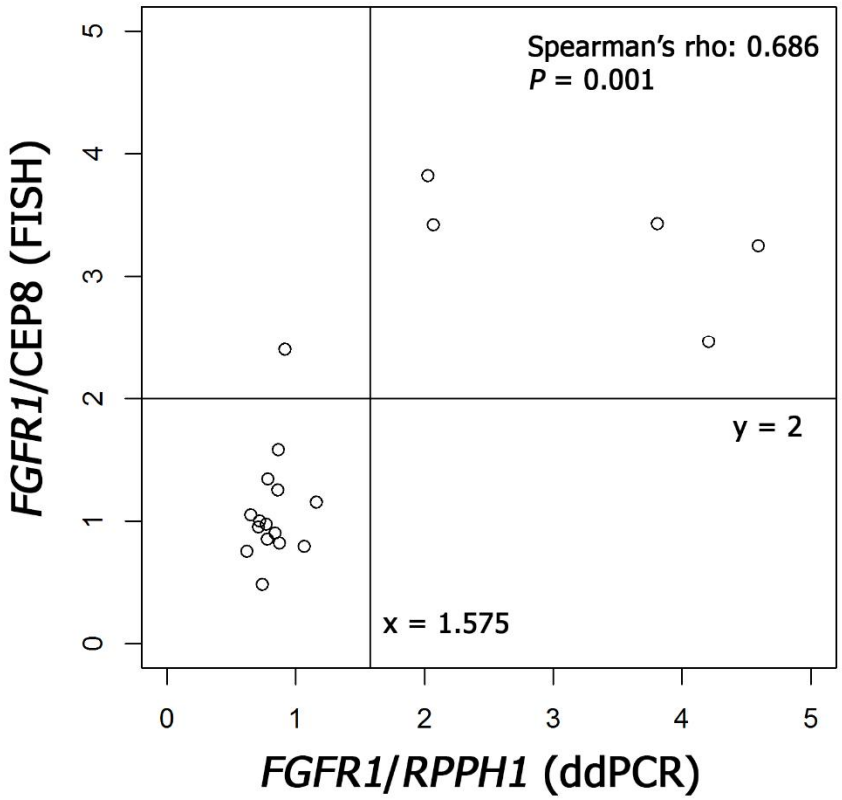

Table 1. *FGFR1* gene status in ddPCR compared with FISH

	FISH	
ddPCR	No-amplification	Amplification
No-amplification	14	1
Amplification	0	5

Patient characteristics

A total of 384 patients with CRC (median age: 63, min – max: 28 – 84) were included in the discovery set. The male to female ratio was 1.42:1 (225 males and 159 females). Tumor location was proximal colon (proximal to the splenic flexure) in 77 patients, distal colon in 143 patients and rectum in 164 patients. Median follow-up duration was 68.8 months. 291 patients received 5-fluorouracil based adjuvant chemotherapy.

In the validation set, a total of 405 patients with high-risk stage II or stage III CRC received adjuvant FOLFOX (median age: 60, min – max: 29 - 78) were included. The male to female ratio was 1.60 (249 males and 156 females). Tumor location was proximal colon in 134 patients, distal colon in 228 patients and rectum in 43 patients. Median follow-up duration was 71.7 months.

Evaluation of *FGFR1* copy number and FGFR1 expression in the discovery set

In the discovery set, median *FGFR1* gene copy number was 1.10 (min - max: 0.15 – 15.00). Using a cut-off of 3.15, 11 patients (2.9%) showed *FGFR1* amplification. By immunohistochemical study, we could obtain FGFR1 expression data of 382

patients from a total of 384 patients. Among 382 patients, 50 patients (13.1%) showed moderate to strong FGFR1 expression while 332 patients (86.9%) showed no to weak FGFR1 expression (Figure 2).

In the validation set, median *FGFR1* gene copy was 1.71 (min - max: 0.35 – 19.20). Thirty-two patients (7.9%) showed FGFR1 amplification. By immunohistochemical study, we could obtain FGFR1 expression data of 375 patients from a total of 405 patients. Among 375 patients, 62 patients (16.5%) showed moderate to strong FGFR1 expression while 313 patients (83.5%) showed no to weak FGFR1 expression.

There was no significant correlation between *FGFR1* copy numbers and FGFR1 expression in the discovery set (*P* for ANOVA = 0.789) and in the validation set (*P* for ANOVA = 0.889) (Figure 3A and B). Also, there was no significant correlation between copy numbers and mRNA expression of *FGFR1* in the TCGA COADREAD dataset (P for ANOVA = 0.561) (Figure 3C)

Figure 2. FGFR1 expression in colorectal cancers. (A) no-expression, (B) mild expression, (C) moderate expression, (D) strong expression.

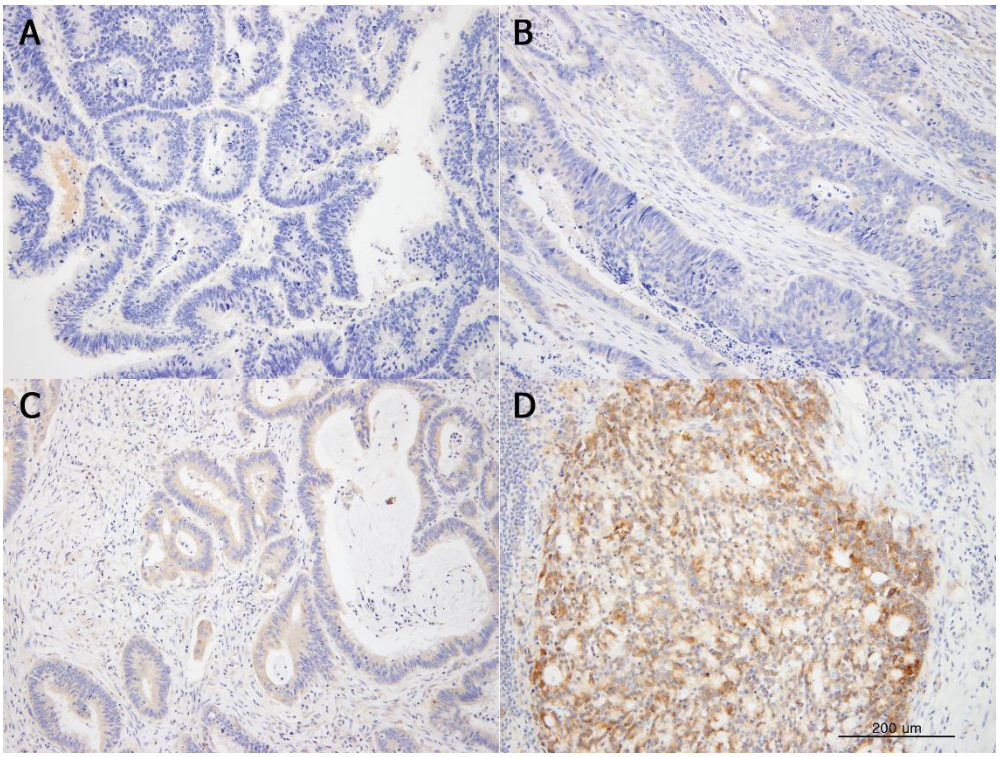

Figure 3. Comparison of *FGFR1* copy and FGFR1 expression in the discovery set and TCGA COADREAD dataset

(A) Discovery set (N = 384)

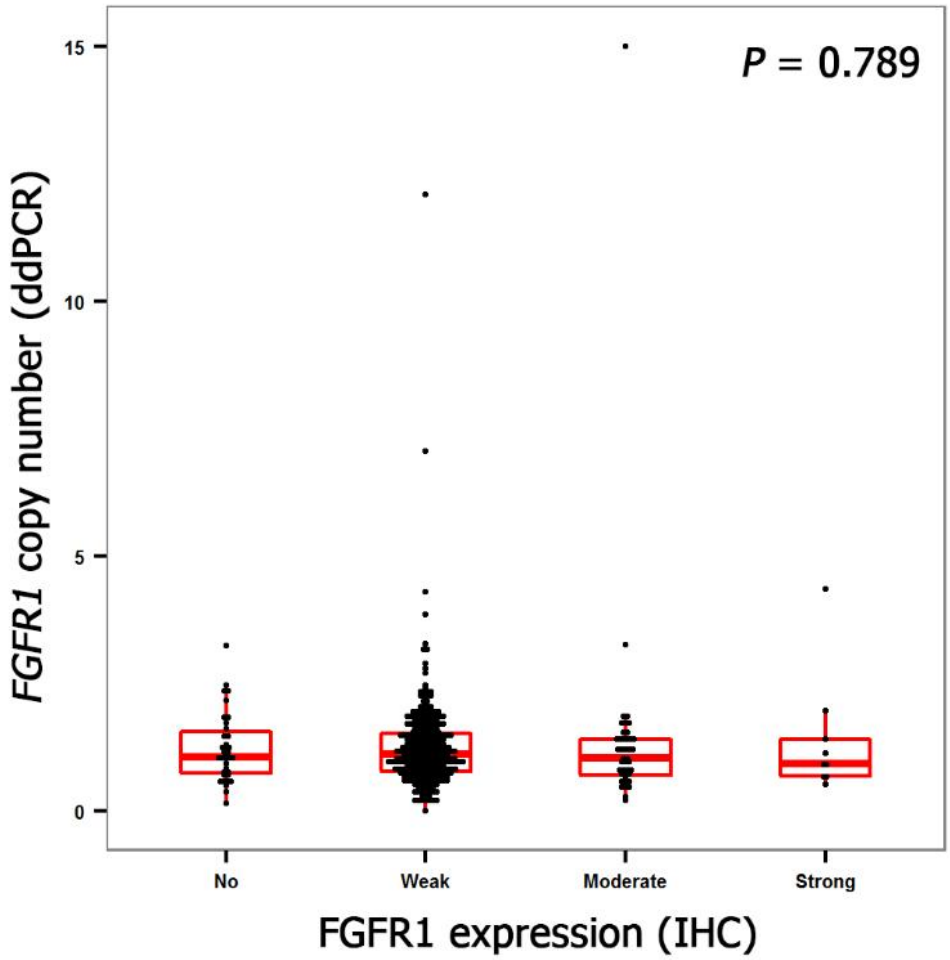

(B) Validation set (N = 405)

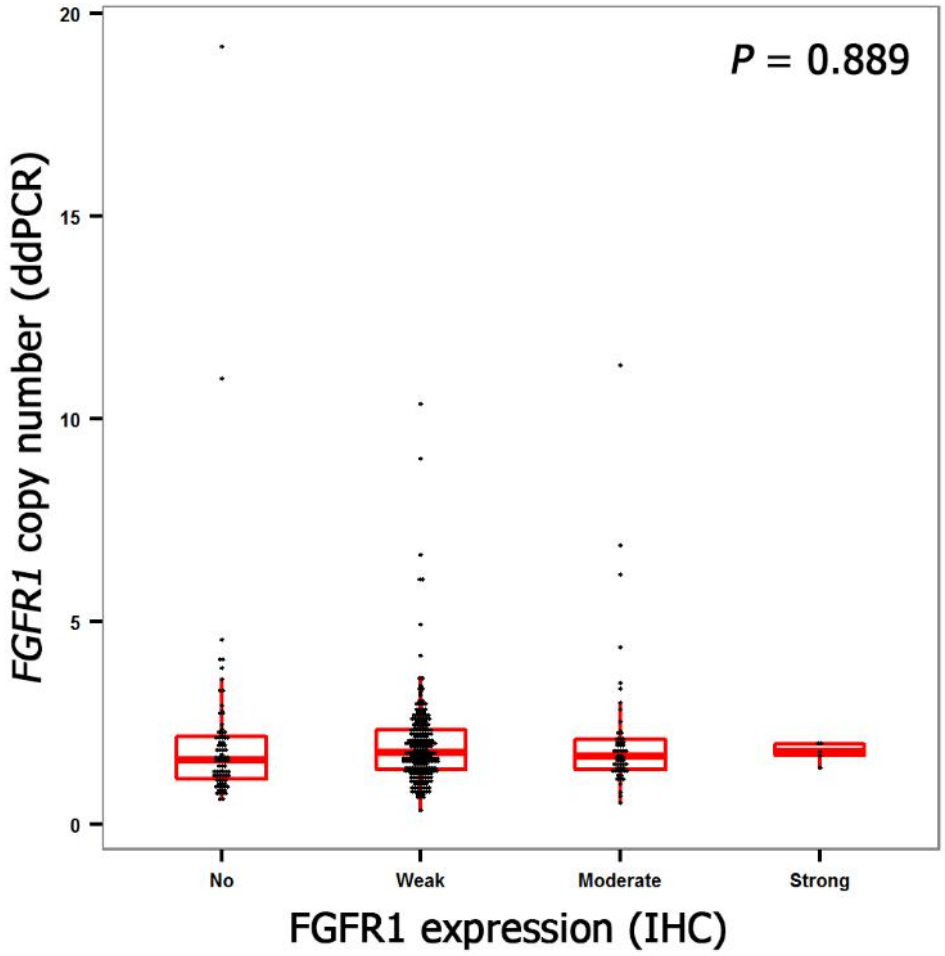

(C) TCGA COADREAD dataset (N = 227)

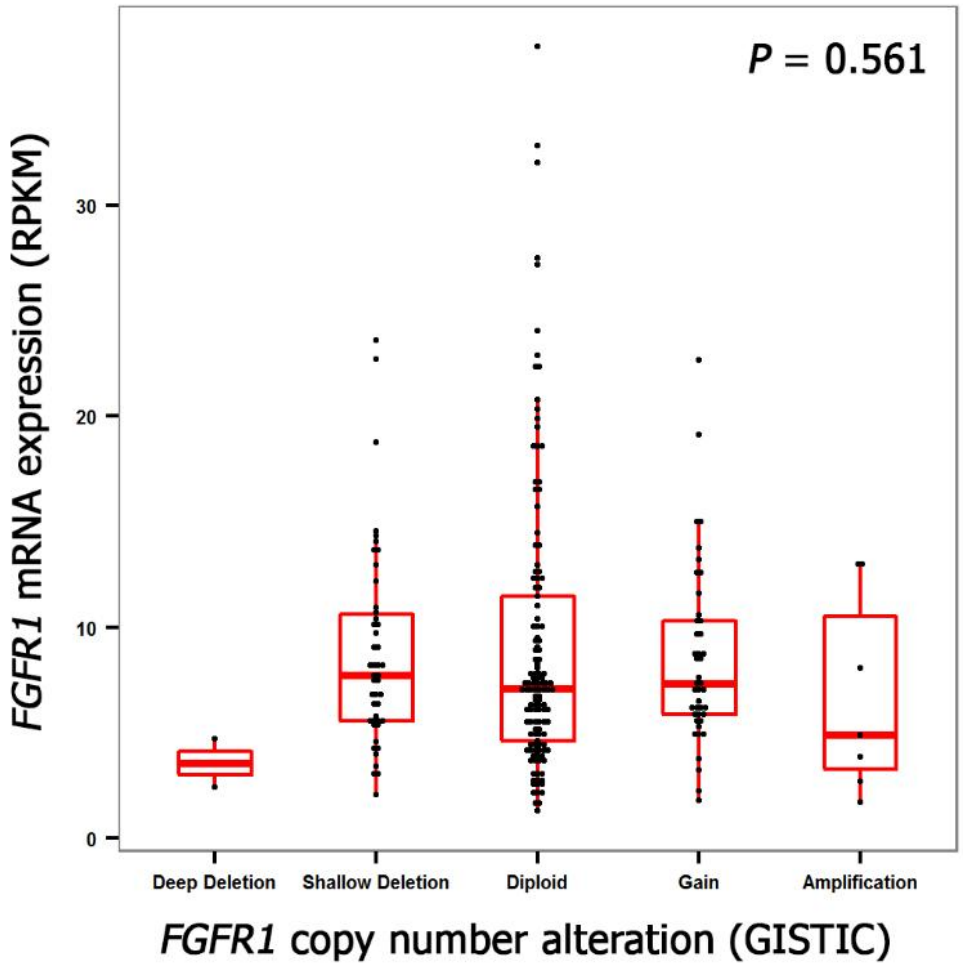

Clinicopathologic characteristics of *FGFR1* amplification and FGFR1 overexpression in the discovery set

Detailed clinicopathologic characteristics of discovery set according to *FGFR1* amplification status in discovery set were summarized in Table 2 and 3. In a clinicopathologic analysis, CRCs with *FGFR1* amplification were marginally associated with lower age of onset (P = 0.046). *FGFR1* amplification showed mutual exclusiveness with MSI-high, CIMP-high and *BRAF* mutation. (Figure 4) Mutual exclusiveness of MSI-high, CIMP-high and *BRAF* mutation with *FGFR1* amplification was also found in TCGA COADREAD dataset.

Detailed clinicopathologic characteristics of discovery set according to FGFR1 expression status in discovery set were summarized in Table 4 and 5. CRCs with FGFR1 high-expression was associated with female preponderance (P = 0.004), advanced N category (P = 0.034) and overall stage (P = 0.018), frequent *KRAS* mutation (P = 0.030), and CIMP-high subtype (P = 0.045) compared with CRCs with FGFR1 low-expression.

Table 2. Clinicopathologic characteristics of CRCs according to the *FGFR1* amplification status in the discovery set (N = 384)

	FGFR1 no-amplification (n = 373, 97.1%)	*FGFR1* amplification (n = 11, 2.9%)	*P*
Age, median (min – max)	63 (28 – 84)	56 (29 – 75)	0.046†
Sex			0.212*
Male	221 (59.2%)	4 (36.4%)	
Female	152 (40.8%)	7 (63.6%)	
Gross pattern			0.756*
Fungating	245 (65.7%)	8 (72.7%)	
Ulcerative	128 (34.3%)	3 (27.3%)	
Tumor location			0.847
Proximal colon	75 (20.1%)	2 (18.2%)	
Distal colon	138 (37.0%)	5 (45.4%)	
Rectum	160 (42.9%)	4 (36.4%)	
T category			0.697*
T1,2	70 (18.8%)	1 (9.1%)	
T3,4	303 (81.2%)	10 (90.9%)	
N category			0.126
N0	189 (50.7%)	3 (27.3%)	
N1,2	184 (49.3%)	8 (72.7%)	
M category			> 0.999*
M0	306 (82.0%)	9 (81.8%)	
M1	67 (18.0%)	2 (18.2%)	
Stage			0.170
I, II	180 (48.3%)	3 (27.3%)	
III, IV	193 (51.7%)	8 (72.7%)	
Differentiation			> 0.999*
Differentiated	360 (96.5%)	11 (100.0%)	
Undifferentiated	13 (3.5%)	0 (0.0%)	

†Wilcoxon's rank-sum test

*Fisher's exact test.

Table 3. Molecular characteristics of CRCs according to the *FGFR1* amplification status in the discovery set (N = 384)

	FGFR1 no-amplification (n = 373, 97.1%)	*FGFR1* amplification (n = 11, 2.9%)	*P*
KRAS mutation			> 0.999*
Wild type	271 (72.6%)	8 (72.7%)	
Mutant type	102 (27.4%)	3 (27.3%)	
BRAF mutation			> 0.999*
Wild type	360 (97.6%)	11 (100.0%)	
Mutant type	9 (2.4%)	0 (0.0%)	
Microsatellite instability			0.709
MSS	319 (85.5%)	10 (90.9%)	
MSI-low	32 (8.6%)	1 (9.1%)	
MSI-high	22 (5.9%)	0 (0.0%)	
CIMP			0.750
CIMP-0	212 (56.8%)	7 (63.6%)	
CIMP-low	145 (38.9%)	4 (36.4%)	
CIMP-high	16 (4.3%)	0 (0.0%)	

*Fisher's exact test.

Figure 4. Mutual exclusiveness of the *FGFR1* amplification with microsatellite instability, *BRAF* mutation and CpG island methylator phenotype

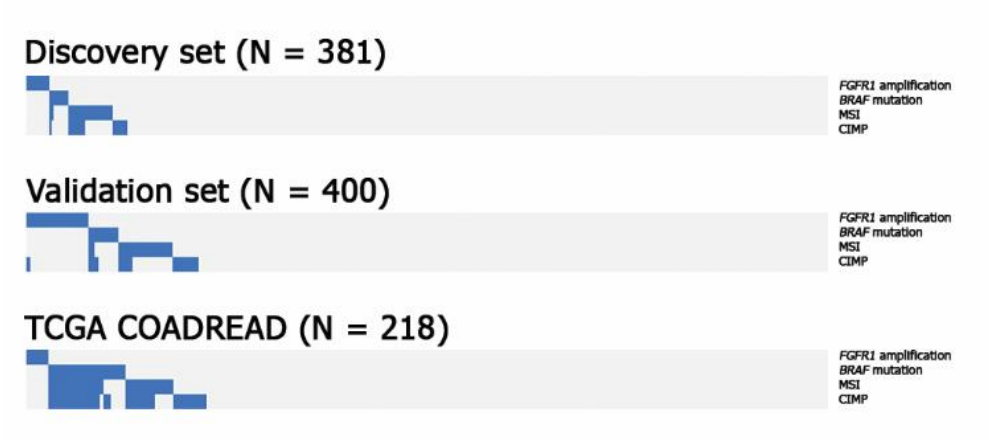

Table 4. Clinicopathologic characteristics of CRCs according to the FGFR1 expression status in the discovery set (N = 382)

	FGFR1 low-expression (n = 332, 86.9%)	FGFR1 high-expression (n = 50, 13.1%)	*P*
Age, median (min – max)	63 (28 – 84)	61 (37 – 83)	0.282†
Sex			0.004
Male	205 (61.7%)	20 (40.0%)	
Female	128 (38.3%)	30 (60.0%)	
Gross pattern			0.339
Fungating	222 (66.9%)	30 (60.0%)	
Ulcerative	110 (33.1%)	20 (40.0%)	
Tumor location			0.272
Proximal colon	63 (19.0%)	14 (28.0%)	
Distal colon	128 (38.5%)	15 (30.0%)	
Rectum	141 (42.5%)	21 (42.0%)	
T category			0.949
T1,2	61 (18.4%)	9 (18.0%)	
T3,4	271 (81.6%)	41 (82.0%)	
N category			0.034
N0	173 (52.1%)	18 (36.0%)	
N1,2	159 (47.9%)	32 (64.0%)	
M category			0.405
M0	275 (82.8%)	39 (78.0%)	
M1	57 (17.2%)	11 (22.0%)	
Stage			0.018
I, II	166 (50.0%)	16 (32.0%)	
III, IV	166 (50.0%)	34 (68.0%)	
Differentiation			> 0.999*
Differentiated	320 (96.4%)	49 (98.0%)	
Undifferentiated	12 (3.6%)	1 (2.0%)	

†Wilcoxon's rank-sum test

*Fisher's exact test.

Table 5. Molecular characteristics of CRCs according to the FGFR1 expression status in the discovery set (N = 382)

	FGFR1 low-expression (n = 332, 86.9%)	FGFR1 high-expression (n = 50, 13.1%)	*P*
KRAS mutation			0.030
Wild type	248 (74.7%)	30 (60.0%)	
Mutant type	84 (25.3%)	20 (40.0%)	
BRAF mutation			0.339*
Wild type	321 (97.9%)	48 (96.0%)	
Mutant type	7 (2.1%)	2 (4.0%)	
Microsatellite instability			0.765
MSS	286 (86.2%)	42 (84.0%)	
MSI-low	28 (8.4%)	4 (8.0%)	
MSI-high	18 (5.4%)	4 (8.0%)	
CIMP			0.045
CIMP-0	194 (58.4%)	23 (46.0%)	
CIMP-low	127 (38.3%)	22 (44.0%)	
CIMP-high	11 (3.3%)	5 (10.0%)	

*Fisher's exact test.

Clinicopathologic and molecular characteristics of *FGFR1* amplification and FGFR1 overexpression in the validation set

Detailed clinicopathologic and molecular characteristics of validation set according to the *FGFR1* amplification status in the validation set were summarized in Table 6. In the validation set, CRCs with *FGFR1* amplification were associated with less frequent *KRAS* mutation (P = 0.021). *FGFR1* amplification showed mutual exclusiveness with MSI-high and *BRAF* mutation, however, 2 out of 32 CRCs with FGFR1 amplification showed CIMP-high (Figure 4).

Detailed clinicopathologic and molecular characteristics of validation set according to the FGFR1 expression status were summarized in Table 7. CRCs with FGFR1 high-expression showed lower stage compared with CRCs with FGFR1 low-expression (P = 0.045). CRCs with FGFR1 high-expression showed tendency of frequent MSI-high and CIMP-high compared with CRCs with FGFR1 low-expression, but statistical significance were marginal (P = 0.083 for MSI, and P = 0.086 for CIMP, respectively).

Table 6. Clinicopathologic and molecular characteristics of CRCs according to the *FGFR1* amplification status in the validation set (N = 405)

	FGFR1 no-amplification (n = 373, 92.1%)	*FGFR1* amplification (n = 32, 7.9%)	*P*
Age, median (min – max)	60 (29 – 78)	56 (42 – 75)	0.089†
Sex			0.902
Male	229 (61.4%)	20 (62.5%)	
Female	144 (38.6%)	12 (37.5%)	
Tumor location			0.023
Proximal colon	129 (34.6%)	5 (15.6%)	
Distal colon	208 (55.8%)	20 (62.5%)	
Rectum	36 (9.6%)	7 (21.9%)	
Stage			0.115*
High-risk stage II	52 (13.9%)	8 (25.0%)	
Stage III	321 (86.1%)	24 (75.0%)	
Differentiation			0.496*
Differentiated	342 (91.7%)	31 (96.9%)	
Undifferentiated	31 (8.3%)	1 (3.1%)	
KRAS (N = 404)			0.021
Wild type	267 (71.8%)	29 (90.6%)	
Mutant type	105 (28.2%)	3 (9.4%)	
BRAF			
Wild type	358 (96.0%)	32 (100.0%)	0.620*
Mutant type	15 (4.0%)	0 (0.0%)	
MSI (N = 400)			0.062
MSS	313 (84.8%)	26 (86.7%)	
MSI-low	26 (7.1%)	5 (16.1%)	
MSI-high	30 (8.1%)	0 (0.0%)	
CIMP			0.969
CIMP-0	226 (60.6%)	19 (59.4%)	
CIMP-low	121 (32.4%)	11 (34.4%)	
CIMP-high	26 (7.0%)	2 (6.2%)	

†Wilcoxon's rank-sum test

*Fisher's exact test

Table 7. Clinicopathologic and molecular characteristics of CRCs according to the FGFR1 expression status in the validation set (N = 375)

	FGFR1 low-expression (n = 313, 83.5%)	FGFR1 high-expression (n = 62, 16.5%)	*P*
Age, median (min – max)	61 (30 – 78)	58 (29 – 76)	0.120†
Sex			0.672
Male	193 (61.7%)	40 (64.5%)	
Female	120 (38.3%)	22 (35.5%)	
Tumor location			0.279
Proximal colon	100 (32.0%)	26 (41.9%)	
Distal colon	176 (56.2%)	31 (50.0%)	
Rectum	37 (11.8%)	5 (8.1%)	
Stage			0.045
High-risk stage II	40 (12.8%)	14 (22.6%)	
Stage III	273 (87.2%)	48 (77.4%)	
Differentiation			0.609*
Differentiated	289 (92.3%)	56 (90.3%)	
Undifferentiated	24 (7.7%)	6 (9.7%)	
KRAS (N = 374)			0.856
Wild type	228 (73.1%)	46 (74.2%)	
Mutant type	84 (26.9%)	16 (25.8%)	
BRAF			0.722*
Wild type	301 (96.2%)	59 (95.2%)	
Mutant type	12 (3.8%)	3 (4.8%)	
MSI (N = 370)			0.083
MSS	262 (84.8%)	48 (78.7%)	
MSI-low	27 (8.7%)	4 (6.6%)	
MSI-high	20 (6.5%)	9 (14.7%)	
CIMP			0.086
CIMP-0	194 (62.0%)	32 (51.6%)	
CIMP-low	101 (32.3%)	22 (35.5%)	
CIMP-high	18 (5.7%)	8 (12.9%)	

†Wilcoxon's rank-sum test

*Fisher's exact test

Survival analysis

In the discovery set, CRC patients with *FGFR1* amplification and FGFR1 high-expression showed worse 5-year progression-free survival in a univariate analysis (P = 0.023 for *FGFR1* amplification and P = 0.022 for FGFR1 high-expression) compared with CRCs with *FGFR1* no-amplification and FGFR1 low-expression, respectively (Figure 5). Because of the scarcity of *FGFR1* amplification in the discovery set, we couldn't perform multivariate survival analysis in the discovery set.

To validate prognostic value of *FGFR1* amplification and FGFR1 high-expression in an independent dataset, we performed survival analysis in a validation set which is stage and adjuvant chemotherapy controlled. In univariate survival analysis, CRCs with *FGFR1* amplification showed marginally worse 5-year disease-free survival (DFS) compared with CRCs with *FGFR1* no-amplification (P = 0.081). 5-year DFS was not significantly different between CRCs with FGFR1 high-expression and CRCs with FGFR1 low-expression (P = 0.337) (Figure 6B). In multivariate survival analysis, *FGFR1* amplification was a prognostic marker of poor 5-year DFS independent of *KRAS* mutation status (Hazard ratio: 2.40, 95% confidence interval: 1.12 – 5.14, P = 0.024) (Figure 6A, Table 8 and 9).

Figure 5. Kaplan-Meier survival curves in the discovery set

(A) 5-year progression-free survival (PFS) according to the *FGFR1* amplification status

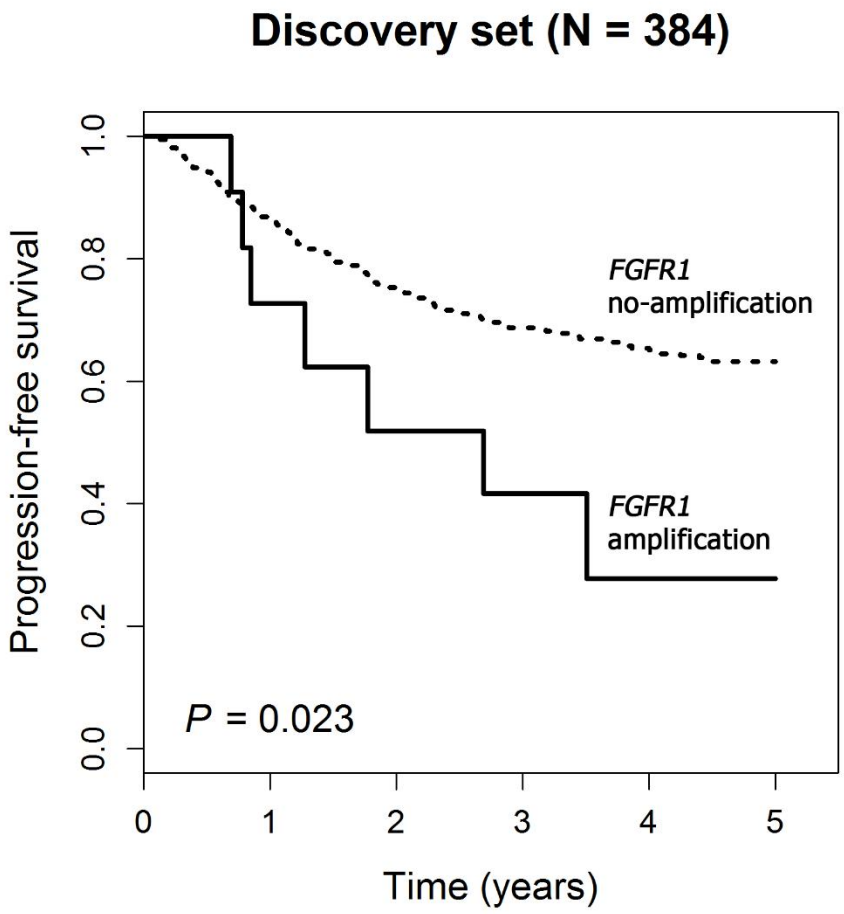

(B) 5-year PFS according to the FGFR1 expression status

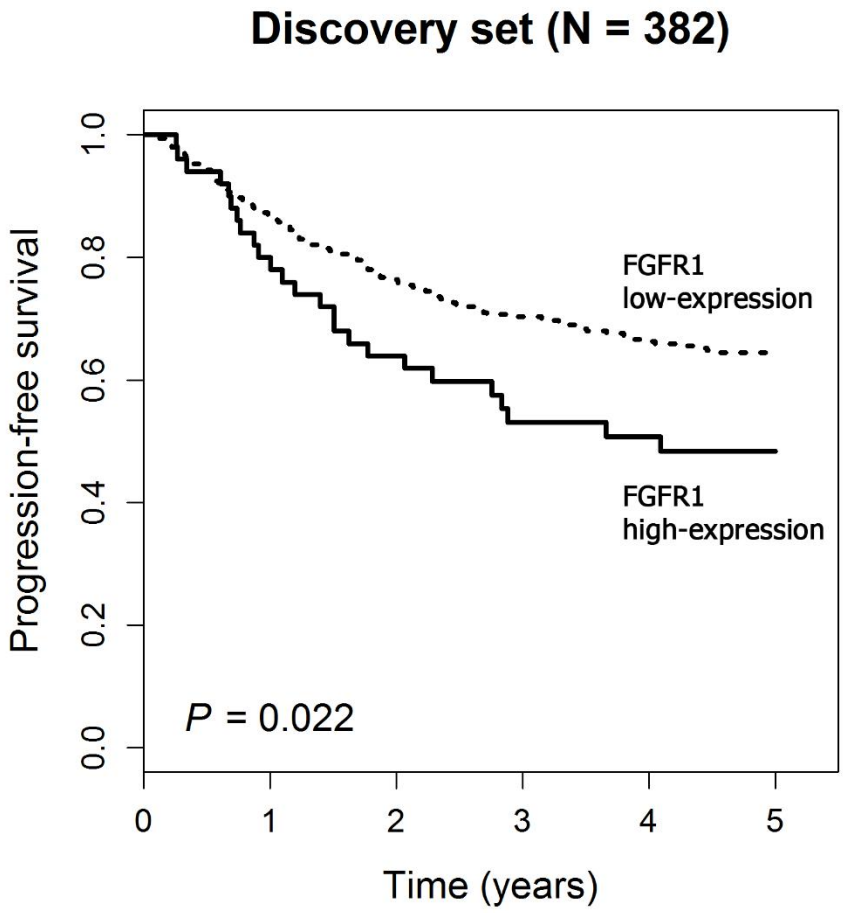

Figure 6. Kaplan-Meier survival curves in the validation set

(A) 5-year disease-free survival according to the *FGFR1* amplification status

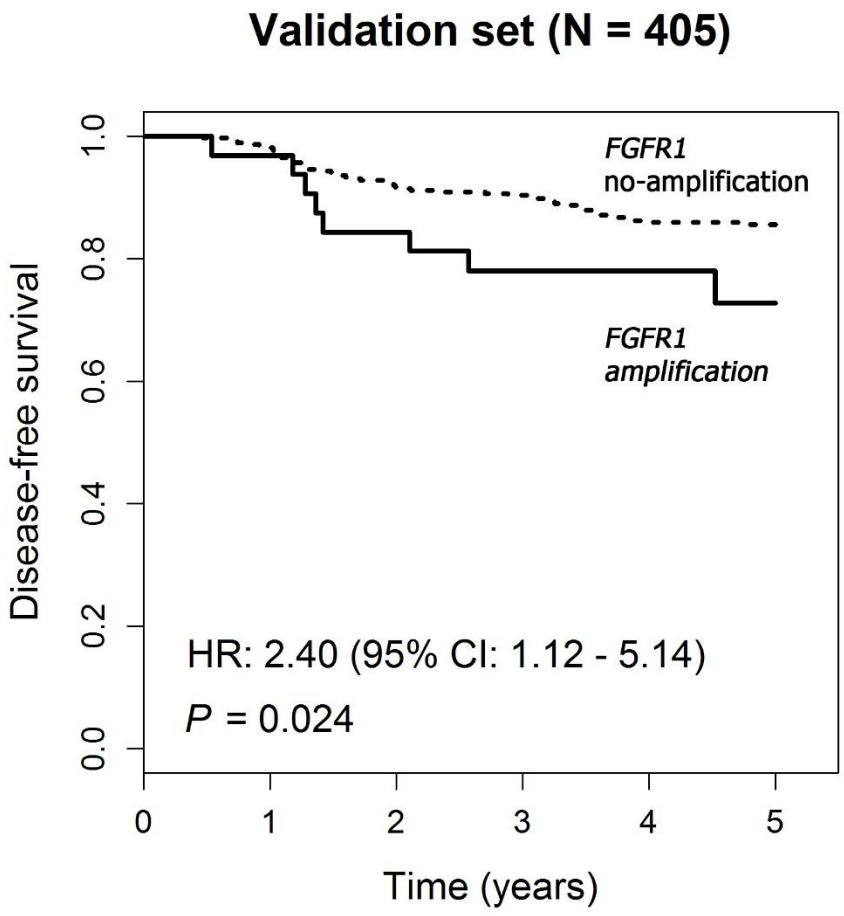

(B) 5-year disease-free survival according to the FGFR1 expression status

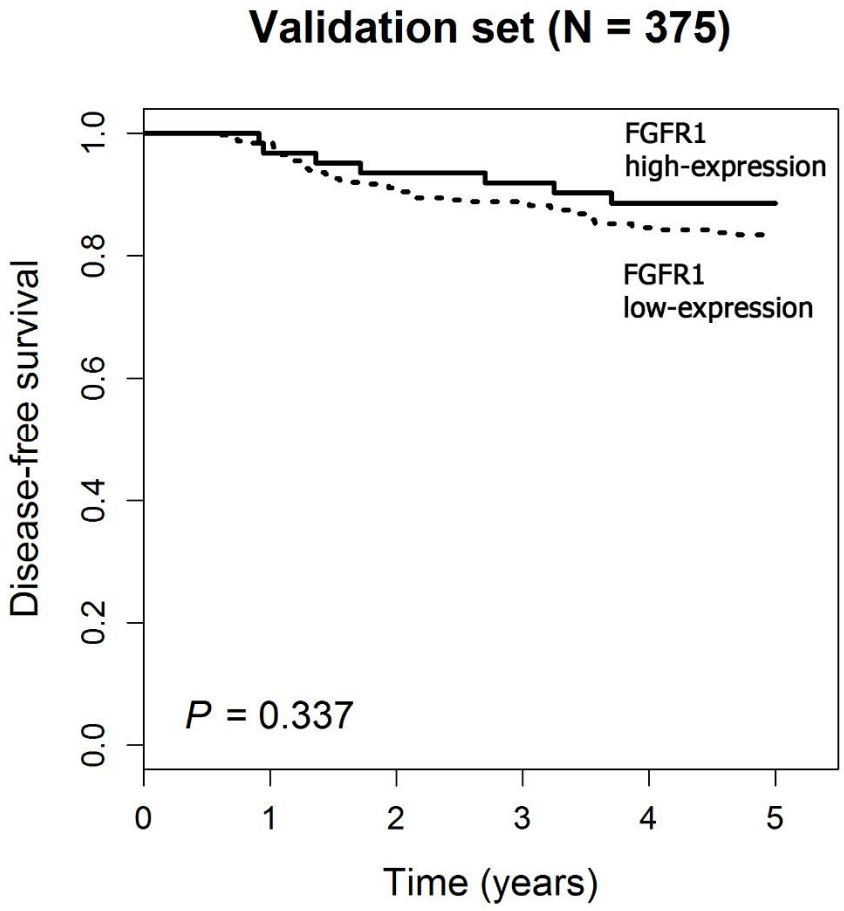

Table 8. Univariate Cox proportional hazard model for 5-year disease-free survival in the validation set (N = 405)

Variables	HR (95% CI)	*P*
KRAS (Mutant type/wild type)	2.18 (1.31 – 3.62)	0.003
FGFR1 CNA (Amplification/no-amplification)	1.94 (0.92 – 4.08)	0.081
FGFR1 expression (High/low)	0.68 (0.31 – 1.50)	0.337
Tumor location (Proximal/Distal, rectum)	0.78 (0.45 – 1.37)	0.395
Age (≥62/<62)	1.37 (0.83 – 2.27)	0.218
Stage (III/high-risk II)	1.15 (0.55 – 2.41)	0.718

Differentiation (Undifferentiated/differentiated)	1.63 (0.74 – 3.58)	0.224
BRAF (Mutant type/wild type)	1.45 (0.46 – 4.64)	0.528
MSI (MSI-high/MSS, MSI-low)	0.93 (0.34 – 2.55)	0.880
CIMP (CIMP-high/CIMP-0, low)	1.58 (0.68 – 3.67)	0.287

Abbreviation: HR, hazard ratio; CI, confidence interval.

Table 9. Multivariate Cox proportional hazard model for 5-year disease-free survival in the validation set (N = 405)

Variables	HR (95% CI)	*P*
KRAS (Mutant type/wild type)	2.38 (1.42 – 4.00)	0.001
FGFR1 (Amplification/no-amplification)	2.40 (1.12 – 5.14)	0.024

Abbreviation: HR, hazard ratio; CI, confidence interval.

FGFR expression status predicts PD173074 sensitivity of CRC cell lines

To investigate whether *FGFR1* amplification or FGFR1 high-expression is a predictive marker for anti-FGFR sensitivity, we performed cell proliferation assay using FGFR1 inhibitor PD173074 on three CRC cell lines with *FGFR1* amplification (SNU-C1, SNU-283 and SW620), one cell line with FGFR1 high-expression (HCT116), and one cell line with FGFR1 no-amplification and FGFR1 low-expression (SNU-81). In cell proliferation assay, PD173074 showed lowest IC_{50} in HCT116 compared with SNU-C1, SNU-283, SW620 and SNU-81 (Figure 7).

Figure 7. IC_{50} of PD173074 in four CRC cell lines

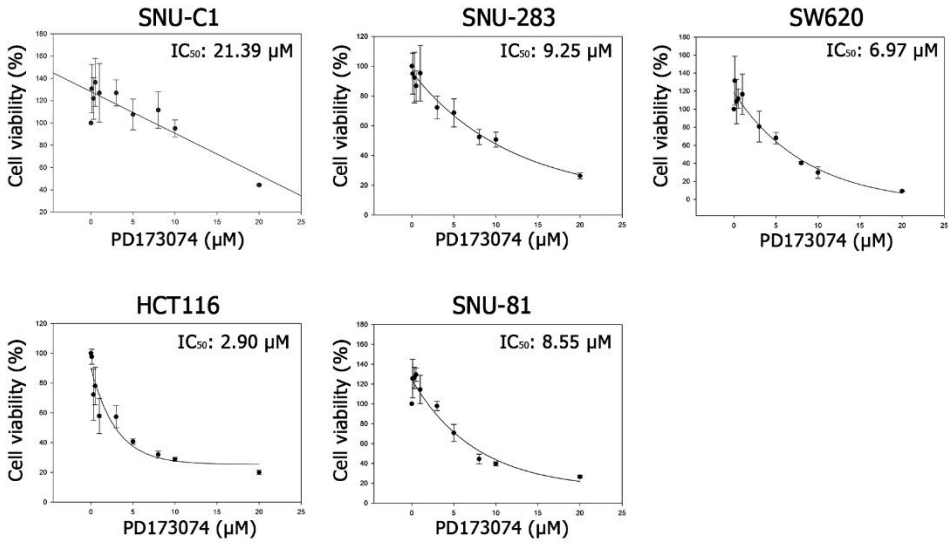

Discussion

PCR is a fundamental method for the detection and quantitation of nucleic acids in the research and clinical diagnostics. The first generation band PCR gives qualitative end-point results on a gel electrophoresis. The second generation real-time PCR enabled quantitation of nucleic acids by monitoring the progression of amplification after each cycle using fluorescence probes. However, real-time PCR has several limitations to clinical diagnostics, such as need for standard curves, expertise skills, and low reproducibility in a quantitation of nucleic acids with low copies. ddPCR is the third generation PCR technology which enables absolute measure of nucleic acid concentration based on limiting dilution, end-point PCR and Poisson statistics.[21] In ddPCR, target DNA molecules are partitioned into 15,000 to 20,000 lipid droplets. After amplification to the terminal plateau phase of PCR, droplets containing one or more templates yield positive end-points, whereas those without template remain negative. The number of target DNA molecules present can be calculated from the fraction of positive end-point reaction using Poisson statistics with following equation: $\lambda = -\ln (1 - P)$, where λ is the average number of target DNA molecules per replicate reaction and P is the fraction of positive end point reactions.[21] Recently, a series of study detected *HER2* amplification successfully in FFPE samples and in plasma DNA of breast cancer

and gastric cancer using ddPCR.[22, 23]

CNA analysis using macro-dissected samples causes underestimation of copy number in *FGFR1* amplified cancers. Because the median tumor cell purity of CRC tissues obtained by manual macro-dissection is about 60%, cut-off of 3.15 for *FGFR1* amplification in ddPCR is equivalent to *FGFR1*/*RPPH1* ratio ≥ 1.96 measured by FISH (0.6 x 1.96 *FGFR1*/*RPPH1* in tumor cells + 0.4 x 1 *FGFR1*/*RPPH1* in normal cells = 3.15/2). *FGFR1*/CEP8 ratio ≥ 2 is accepted for a cut-off of *FGFR1* amplification in various type of cancers.[9, 24-26] Therefore, cut-off of 3.15 for *FGFR1* amplification in macro-dissected samples could be acceptable for the evaluation of *FGFR1* amplification.

Little is known about the clinicopathologic characteristics of CRCs with *FGFR1* gene amplification. In our present study, CRCs with *FGFR1* amplification showed marginally younger age at diagnosis in the discovery set. TNM stage and tumor differentiation were not significantly different between *FGFR1* not-amplified group and *FGFR1* amplified group. In a molecular analysis, *FGFR1* amplification showed mutual exclusiveness with MSI, CIMP and *BRAF* mutation in the discovery set, and with MSI and *BRAF* mutation in the validation set. This mutual exclusiveness was constantly replicated in the TCGA COADREAD dataset. These results suggested that *FGFR1* amplification in CRCs occurs in the context of chromosomal instability, rather than microsatellite instability or CIMP.

Several pharmacological agents have been developed to inhibit FGFR activity. These include multi-target receptor tyrosine kinase inhibitor showing efficacy to VEGFR, PDGFR and FGFR, and selective FGFR inhibitor which suppress FGFR1-3.[27] Non-selective broad-spectrum receptor tyrosine kinase inhibitors showed only modest bioactivity against FGFR and wide-spectrum off-target effect.[28] Selective FGFR inhibitors, such as AZD4547 and BGJ398 showed tolerable side effects, however, did not fulfilled pre-specified efficacy endpoint in phase 1 clinical trials.[29-31] Furthermore, it is still controversial whether *FGFR1* amplification or overexpression is an appropriate biomarker for anti-FGFR therapy. Weiss et al. showed that selective FGFR inhibitor PD173074 inhibited growth and induced apoptosis in lung cancer cells carrying *FGFR1* amplification.[32] However, in our present study, PD173074 showed lowest IC50 in HCT116 cell line exhibiting high *FGFR1* expression. Furthermore, BGJ398 and AZD4547 showed strong anti-proliferative effect in CRC cell lines exhibiting high *FGFR1* expression.[17, 18] Proper selection of biomarker which can predict response to FGFR targeted therapy is required.

Conclusion

FGFR1 amplification is a prognostic indicator of poor clinical outcome in CRCs. Evaluation of somatic CNA using ddPCR can be an alternative diagnostic method to FISH for clinical diagnostics.

References

1. Siegel, R.L., K.D. Miller, and A. Jemal, *Cancer statistics, 2016.* CA Cancer J Clin, 2016. **66**(1): p. 7-30.
2. Oh, C.M., et al., *Cancer Statistics in Korea: Incidence, Mortality, Survival, and Prevalence in 2013.* Cancer Res Treat, 2016. **48**(2): p. 436-50.
3. Network, T.C.G.A., *Comprehensive molecular characterization of human colon and rectal cancer.* Nature, 2012. **487**(7407): p. 330-7.
4. Fearon, E.R. and B. Vogelstein, *A genetic model for colorectal tumorigenesis.* Cell, 1990. **61**(5): p. 759-67.
5. Ciriello, G., et al., *Emerging landscape of oncogenic signatures across human cancers.* Nat Genet, 2013. **45**(10): p. 1127-33.
6. Dienstmann, R., et al., *Genomic aberrations in the FGFR pathway: opportunities for targeted therapies in solid tumors.* Ann Oncol, 2014. **25**(3): p. 552-63.
7. Turner, N. and R. Grose, *Fibroblast growth factor signalling: from development to cancer.* Nat Rev Cancer, 2010. **10**(2): p. 116-29.
8. Kim, H.R., et al., *Fibroblast growth factor receptor 1 gene amplification is associated with poor survival and cigarette smoking dosage in patients with resected squamous cell lung cancer.* J Clin Oncol, 2013. **31**(6): p. 731-7.
9. Kim, H.S., et al., *Fibroblast growth factor receptor 1 gene amplification is associated with poor survival in patients with resected esophageal squamous cell carcinoma.* Oncotarget, 2015. **6**(4): p. 2562-72.
10. Elbauomy Elsheikh, S., et al., *FGFR1 amplification in breast carcinomas: a chromogenic in situ hybridisation analysis.* Breast Cancer Res, 2007. **9**(2): p. R23.
11. Cappuzzo, F., et al., *Epidermal growth factor receptor gene and protein*

and gefitinib sensitivity in non-small-cell lung cancer. J Natl Cancer Inst, 2005. **97**(9): p. 643-55.

12. Wolff, A.C., et al., *Recommendations for human epidermal growth factor receptor 2 testing in breast cancer: American Society of Clinical Oncology/College of American Pathologists clinical practice guideline update.* J Clin Oncol, 2013. **31**(31): p. 3997-4013.
13. Fritzsche, F.R., et al., *Determination of the Her-2/neu gene amplification status in cytologic breast cancer specimens using automated silver-enhanced in-situ hybridization (SISH).* Am J Surg Pathol, 2010. **34**(8): p. 1180-5.
14. Yoo, S.B., et al., *Reliability of chromogenic in situ hybridization for epidermal growth factor receptor gene copy number detection in non-small-cell lung carcinomas: a comparison with fluorescence in situ hybridization study.* Lung Cancer, 2010. **67**(3): p. 301-5.
15. Huggett, J.F., S. Cowen, and C.A. Foy, *Considerations for digital PCR as an accurate molecular diagnostic tool.* Clin Chem, 2015. **61**(1): p. 79-88.
16. Nakao, K., et al., *High-resolution analysis of DNA copy number alterations in colorectal cancer by array-based comparative genomic hybridization.* Carcinogenesis, 2004. **25**(8): p. 1345-57.
17. Goke, F., et al., *Fibroblast growth factor receptor 1 as a putative therapy target in colorectal cancer.* Digestion, 2013. **88**(3): p. 172-81.
18. Yao, T.J., et al., *AZD-4547 exerts potent cytostatic and cytotoxic activities against fibroblast growth factor receptor (FGFR)-expressing colorectal cancer cells.* Tumour Biol, 2015. **36**(7): p. 5641-8.
19. Cerami, E., et al., *The cBio cancer genomics portal: an open platform for exploring multidimensional cancer genomics data.* Cancer Discov, 2012. **2**(5): p. 401-4.
20. Kwak, Y., et al., *Fibroblast Growth Factor Receptor 1 Gene Copy Number and mRNA Expression in Primary Colorectal Cancer and Its Clinicopathologic Correlation.* Pathobiology, 2015. **82**(2): p. 76-83.
21. Hindson, B.J., et al., *High-throughput droplet digital PCR system for*

absolute quantitation of DNA copy number. Anal Chem, 2011. **83**(22): p. 8604-10.

22. Kinugasa, H., et al., *Droplet digital PCR measurement of HER2 in patients with gastric cancer.* Br J Cancer, 2015. **112**(10): p. 1652-5.
23. Zhu, Y., et al., *Droplet digital polymerase chain reaction detection of HER2 amplification in formalin fixed paraffin embedded breast and gastric carcinoma samples.* Exp Mol Pathol, 2016. **100**(2): p. 287-93.
24. Zhang, L., et al., *Fibroblast Growth Factor Receptor 1 and Related Ligands in Small-Cell Lung Cancer.* J Thorac Oncol, 2015. **10**(7): p. 1083-90.
25. Tran, T.N., et al., *Fibroblast growth factor receptor 1 (FGFR1) copy number is an independent prognostic factor in non-small cell lung cancer.* Lung Cancer, 2013. **81**(3): p. 462-7.
26. Koole, K., et al., *FGFR1 Is a Potential Prognostic Biomarker and Therapeutic Target in Head and Neck Squamous Cell Carcinoma.* Clin Cancer Res, 2016.
27. Shaw, A.T., et al., *Tyrosine kinase gene rearrangements in epithelial malignancies.* Nat Rev Cancer, 2013. **13**(11): p. 772-87.
28. Lewin, J. and L.L. Siu, *Development of Fibroblast Growth Factor Receptor Inhibitors: Kissing Frogs to Find a Prince?* J Clin Oncol, 2015. **33**(30): p. 3372-4.
29. Paik, P.K., et al., *A phase 1b open-label multicenter study of AZD4547 in patients with advanced squamous cell lung cancers: Preliminary antitumor activity and pharmacodynamic data.* ASCO Meeting Abstracts, 2014. **32**(15_suppl): p. 8035.
30. Arkenau, H.-T., et al., *A phase 1 expansion cohort of the fibroblast growth factor receptor (FGFR) inhibitor AZD4547 in patients (pts) with advanced gastric (GC) and gastroesophageal (GOJ) cancer.* ASCO Meeting Abstracts, 2014. **32**(15_suppl): p. 2620.
31. Nogova, L., et al., *Targeting FGFR1-amplified lung squamous cell carcinoma with the selective pan-FGFR inhibitor BGJ398.* J Clin Oncol (Meeting Abstracts), 2014. **32**(15_suppl): p. 8034-.

32. Weiss, J., et al., *Frequent and focal FGFR1 amplification associates with therapeutically tractable FGFR1 dependency in squamous cell lung cancer.* Sci Transl Med, 2010. **2**(62): p. 62ra93.

국문초록

제1형 섬유모세포성장인자수용체(*Fibroblast growth factor receptor 1*, *FGFR1*) 유전자의 증폭이 다수의 종양에서 보고되었다. 그러나 결장직장암에서 *FGFR1* 유전자의 증폭이 갖는 임상병리학적 특징과 예후에 미치는 영향에 대해서는 알려진 바가 거의 없는 실정이다. 본 연구는 384례의 발굴군과 405례의 검증군을 포함한 총 789례의 결장직장암 조직에서 비말 디지털 중합효소연쇄반응(droplet digital polymerase chain reaction, ddPCR) 기법을 이용하여 *FGFR1* 유전자의 복제수 변이를 측정하고, 면역조직화학염색 기법을 통하여 FGFR1 유전자의 단백질 발현을 측정하였다. *FGFR1* 유전자 증폭은 복제수 3.15 이상을 기준으로 하였다.

FGFR1 유전자 증폭은 384례의 발굴군 중 2.9%인 11례에서 발견되었고, 405례의 검증군 중 7.9%인 32례에서 발견되었다. FGFR1 유전자 증폭은 미소부수체불안정, *BRAF* 유전자 돌연변이와 상호배타성을 나타내었다. *FGFR1* 유전자 복제수에 따른 성별, 종양의 육안형, 종양의 위치, 병기와 분화도의 차이는 발견되지 않았다. FGFR1 단백의 과발현은 382례의 발굴군 중 13.1%인 50례에서 발견되었고,

375례의 검증군 중 16.5%인 62례에서 발견되었다. FGFR1 유전자 증폭과 FGFR1 단백의 과발현 간 유의한 상관관계를 보이지 않았다. 발굴군에서 FGFR1 단백의 과발현은 여성에서 호발하였으며, 림프절 전이, 높은 병기, *KRAS* 유전자 돌연변이와 CpG island 메틸화 아형과 관련을 보였다. 생존분석에서 *FGFR1* 유전자 증폭 환자군은 발굴군과 검증군 모두에서 *FGFR1* 유전자 증폭이 없는 환자군에 비하여 불량한 예후를 보였으나, FGFR1 단백의 과발현 환자군은 발굴군에서만 FGFR1 단백의 저발현 환자군에 비하여 불량한 예후를 나타내었다. FGFR 억제제인 PD173074를 결장직장암 세포주에 처리하였을 때 FGFR1 단백이 과발현되는 세포주에서 FGFR1 유전자 증폭이 관찰되는 세포주에 비하여 낮은 IC50 값을 나타내었다.

결론적으로, 비말 디지털 중합효소연쇄반응 기법으로 측정한 FGFR1 유전자의 증폭은 결장직장암 환자의 불량한 예후를 예측할 수 있는 예후 인자로 사용될 수 있을 것으로 기대된다.